

## Electron-Induced (EI) Mass Fragmentation is Directed by Intramolecular H-Bonding in Two Isomeric Benzodipyran Systems

Cornelis J. Van der Schyf<sup>1,2,\*</sup> and Stéphane Mabic<sup>3</sup>

<sup>1</sup> Department of Pharmaceutical Sciences, Texas Tech University Health Sciences Center, School of Pharmacy, Amarillo, TX 79106, USA. Tel. +1 (806) 356-4015 xt. 329, Fax +1 (806) 356-4034.

<sup>2</sup> School of Pharmacy, North West University, Potchefstroom 2520, South Africa.

<sup>3</sup> Research and Development, Lab Water Division, Millipore, St Quentin-Yvelines, France.

\* Author to whom correspondence should be addressed; e-mail: neels.vanderschyf@ttuhsc.edu

Received: 30 March 2004 / Accepted: 29 July 2004 / Published: 30 September 2004

---

**Abstract:** The striking differences observed in the electron-induced (EI) mass fragmentation pathways of two isomeric benzodipyrans are attributable to hydrogen bonding in these molecules. In the "angular" isomer, 6-butyryl-5-hydroxy-2,2,8,8-tetramethyl-3,4,9,10-tetrahydro-2H,8H-benzo[1,2-b:3,4-b<sup>1</sup>]dipyran (**2**), H-bonding occurs between the aromatic OH group and the *alpha* carbonyl moiety contained in the *ortho*-phenone group, whereas in the "linear" isomer, 10-butyryl-5-hydroxy-2,2,8,8-tetramethyl-3,4,6,7-tetrahydro-2H,8H-benzo[1,2-b:5,4-b<sup>1</sup>]dipyran (**3**), the aromatic OH group is *para* to the phenone moiety, effectively precluding any H-bonding. Semi-empirical molecular orbital calculations (AM1) were used to compare predicted sites of ionization with associated fragmentation patterns. In both molecules, the highest occupied molecular orbital (HOMO) was located predominantly on the aromatic moiety. Similarly, in the radical cation species of both compounds, maximum spin density was located over the aromatic rings. Neither the HOMO nor the spin density maps provided a rational explanation for the differences in fragmentation patterns of the two benzodipyran isomers. The H-bonding favors EI *alpha* aromatic ring C-O bond cleavage in the "angular" benzodipyran and in 5,7-dihydroxy-2,2-dimethyl-8-butyryl chroman (**1**), a related monochroman also containing a hydrogen proximal to the aromatic ring C-O bond. In contrast, fragmentation of the "linear" benzodipyran followed a different route, which was exhibited by its base peak resulting from the loss of a propyl group from the butyryl side-chain.

**Keywords:** benzodipyrans, hydrogen-bond directed mass fragmentation, EIMS.

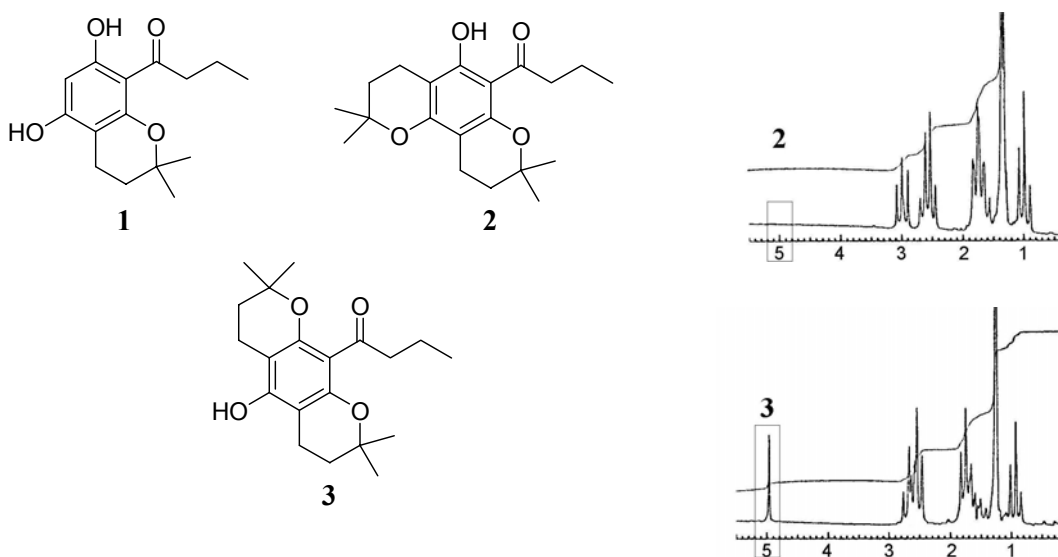
---

## Introduction

Early investigations into the potentially useful pharmacological properties of chroman and benzodipyran derivatives focused primarily on their antiallergic [1] and antimicrobial [2] activities. A resurgence of interest in these compounds since the early 1990s explored their utility across a broad spectrum of activities such as anticancer agents with low toxicity [4], anti-inflammatory agents [5], potassium channel openers with possible cardioprotective properties [6,7], and agonists at serotonergic 5-HT<sub>1A</sub> receptors [8].

It is therefore not surprising that the EI mass spectrometry (EIMS) of chroman derivatives has been studied extensively [9–14]. Due to earlier work [2] with the 2,2-dimethylchroman (5,7-dihydroxy-2,2-dimethyl-8-butyryl chroman) **1** and benzodipyran derivatives **2** and **3** (Figure 1), the mass spectrometry of related compounds was of particular interest to us. We proceeded to study these compounds with simple EIMS and low resolution NMR.

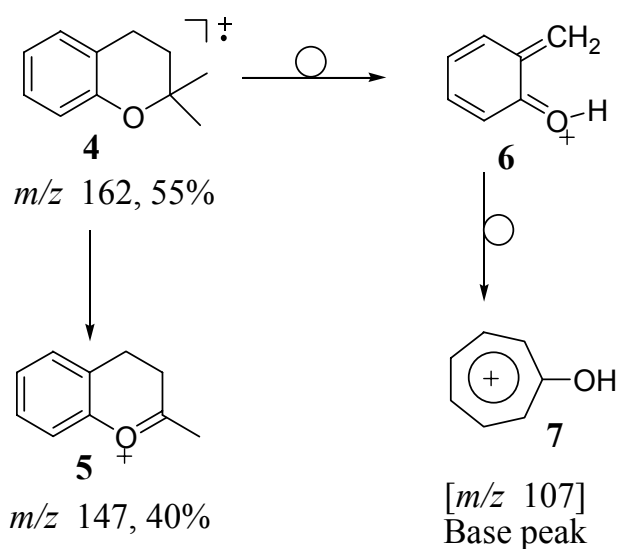
**Figure 1.** Structures of compounds discussed in the text: 5,7-dihydroxy-2,2-dimethyl-8-butyryl chroman (**1**), the "angular" benzodipyran isomer **2** and the "linear" benzodipyran isomer **3**; (right) 80 MHz NMR spectra of **2** and **3** respectively, showing the exchangeable phenolic proton signal at 4.95 ppm in the case of **3**.



The EIMS of 2,2-dimethylchroman **4** (Scheme 1) was shown [9,10] to proceed via two main fragmentation pathways. The first pathway involved the loss of a methyl group (major fragment) followed by either the loss of ethylene or the second methyl group (minor fragments). The fragment ion **5** at  $m/z$  147 (corresponding to the loss of a methyl group) is prominent (40% intensity) in the EI mass spectrum (Scheme 1). The other fragmentation pathway proceeds via loss of a  $[\text{CH}_2=\text{C}(\text{CH}_3)\text{CH}_2]$  fragment (55 amu) and is accompanied by transfer of a hydrogen to the oxygen atom, giving rise to the base peak **6** at  $m/z$  107. The protonated quinone methide intermediate **6** rearranges to a more stable

tropylium ion **7**. The details of the fragmentation as well as the origins of the carbons and the hydrogens in the fragment ions were elegantly elucidated by Trudell *et al.* [10] through analogs regioselectively labeled with deuterium and  $^{13}\text{C}$ . Further discussions detailing these aspects will not be elaborated within this report. Rather, the focus of this paper will be to offer explanations for the striking differences observed in the fragmentation patterns reported for 2,2-dimethylchroman **4** and those of the three chroman derivatives **1**, **2** and **3** synthesized by us (see Figure 1). Additionally, a rational explanation is presented for the drastic differences in the fragmentation patterns of the two benzodipyrans, the "linear" and "angular" isomers, **2** and **3**, respectively.

**Scheme 1.** EI fragmentation of 2,2-dimethylchroman **4** (intensities are indicated in % relative to the base peak).



## Results and Discussion

The monochroman, 5,7-dihydroxy-2,2-dimethyl-8-butyryl chroman (**1**) exhibits two major fragmentation pathways (Scheme 2). The first proceeds via cleavage that occurs  $\beta$  to the aromatic moiety yielding molecular ion **8** at *m/z* 221 corresponding to the loss of the propyl group (43 amu) (Figure 2) followed by a retro Diels-Alder rearrangement of the chroman moiety to give the quinone methide ion **9** at *m/z* 165. This intermediate most likely rearranges to a more stable oxotropylium ion **10**, as previously described for **4** [10]. The stable oxotropylium ion constitutes the base peak of the spectrum. The retro Diels-Alder rearrangement occurs without hydrogen transfer to the oxygen atom, and thus results in the loss of the  $[\text{CH}_2=\text{C}(\text{CH}_3)_2]$  fragment (56 amu). The second major pathway proceeds by fragmentation of the chroman with hydrogen transfer to the oxygen and loss of a fragment of 55 amu. This loss yields a fragment ion **11** at *m/z* 209, which likely rearranges to the more stable tropylium ion **12**. Cleavage  $\alpha$  to the aromatic ring and loss of a  $[\text{CO-propyl}]$  fragment to yield the chromandiol species **13** at *m/z* 193 (17% intensity) is also observed. However, it was not determined whether this loss occurs stepwise from

ion **8** or directly from the parent ion **1**<sup>+</sup>. Of interest is that in contrast to the fragmentation pattern reported for **4**, no loss of a methyl group from the chroman moiety is observed in this spectrum.

**Scheme 2.** EI fragmentation of 5,7-dihydroxy-2,2-dimethyl-8-butyryl chroman (**1**).

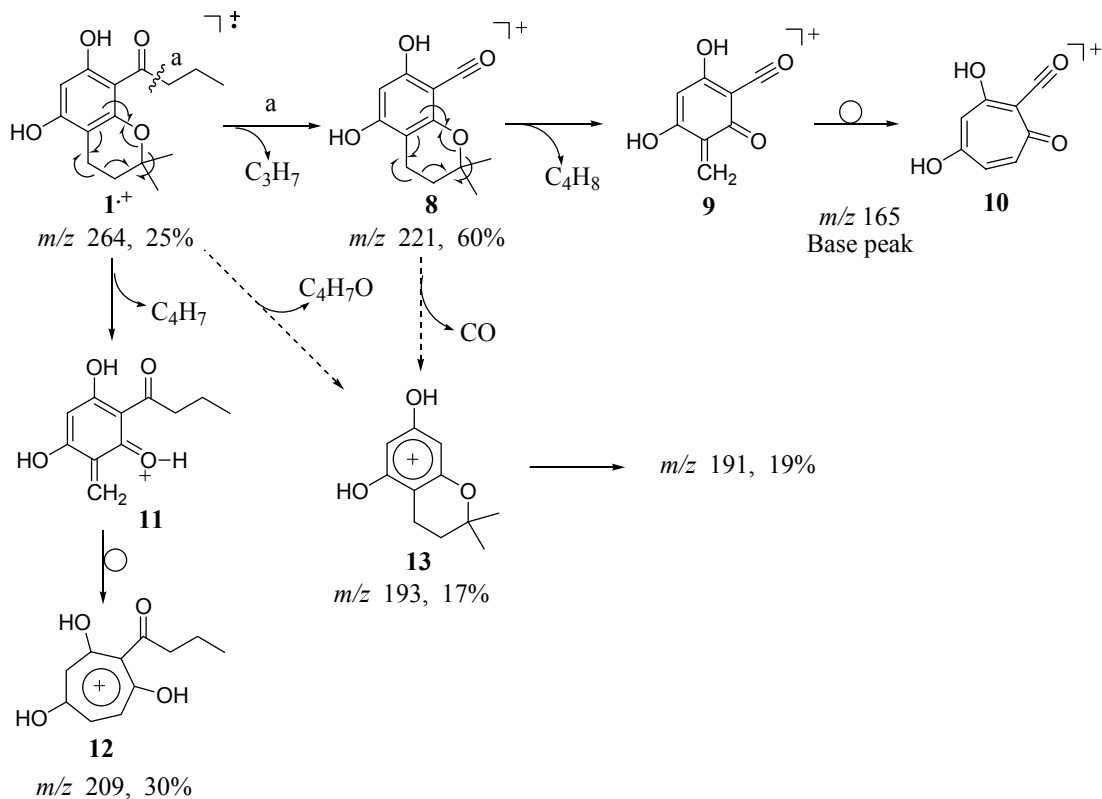
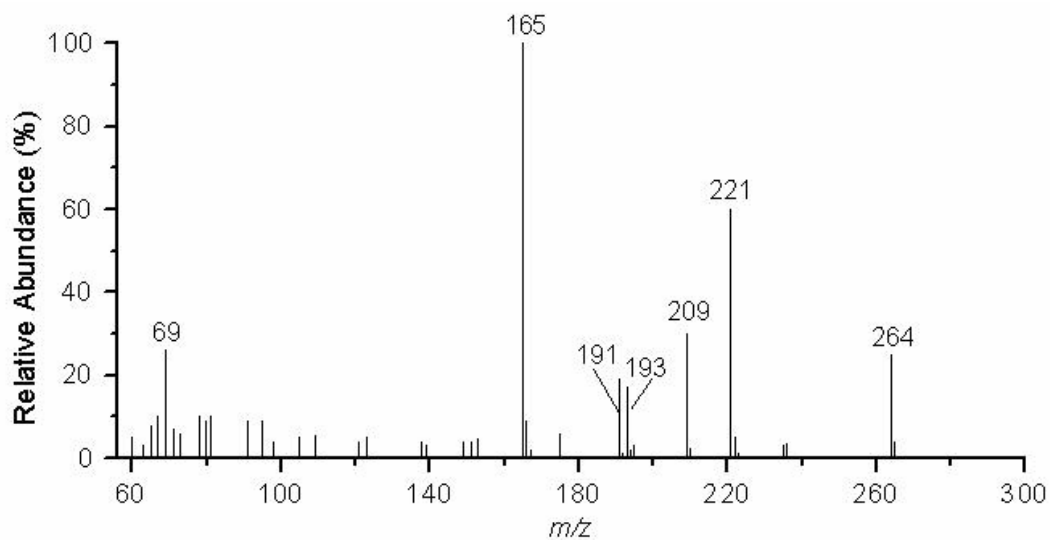
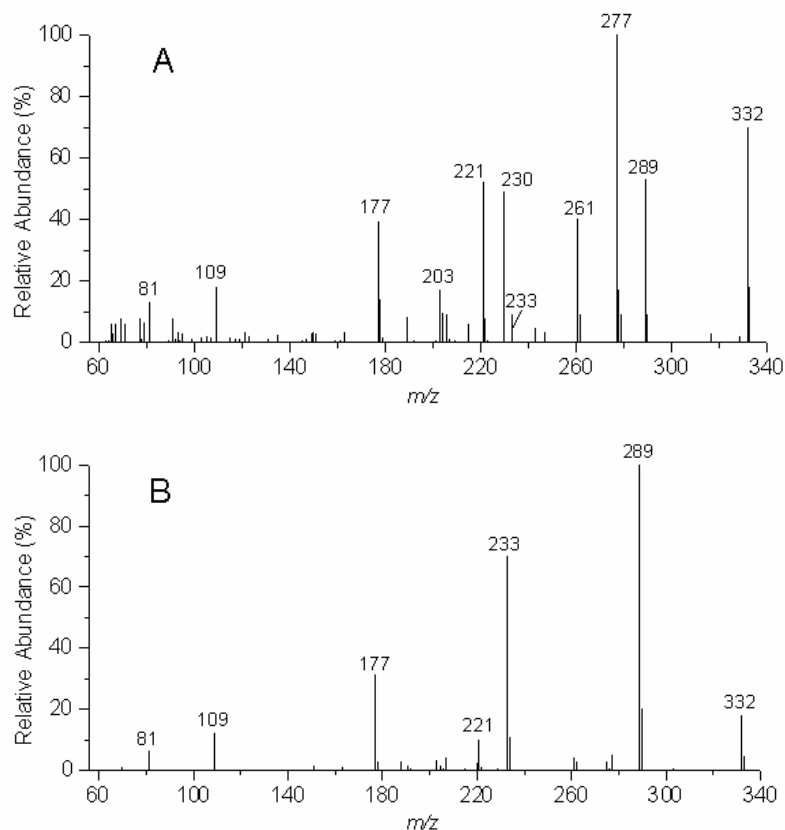


**Figure 2.** EIMS (70 eV) of 5,7-dihydroxy-2,2-dimethyl-8-butyryl chroman (**1**).



There are striking differences in the EIMS fragmentation patterns of the two isomeric benzodipyrans, **2** and **3** (see Figures 3A and 3B and Table 1). While loss of a fragment of 55 amu gives rise to the base peak fragment for **2**, the cleavage  $\beta$  to the aromatic ring to render the characteristic  $\text{Ar-C}\equiv\text{O}^+$  fragment **15** at  $m/z$  289 constitutes the base peak for **3**. (See Table 1). As discussed above, this fragment of 55 amu is typically observed in the EIMS of 2,2-dimethylchromans and accounts for the loss of the  $[\text{CH}_2=\text{C}(\text{CH}_3)\text{CH}_2]$  fragment in a retro Diels-Alder rearrangement and the proton transfer to the oxygen atom (Scheme 1 and 2) [9,10].

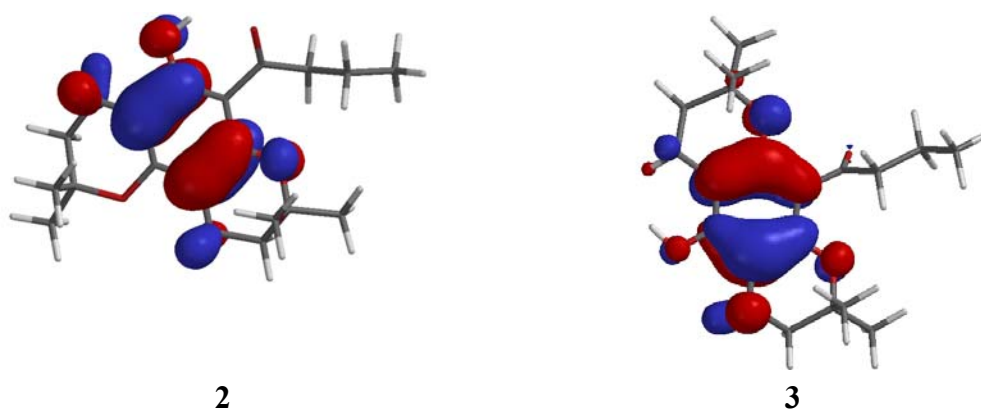
**Figure 3.** EIMS (70 eV) of the "angular" benzodipyrans **2** (A, upper panel) and the "linear" benzodipyrans **3** (B, lower panel).

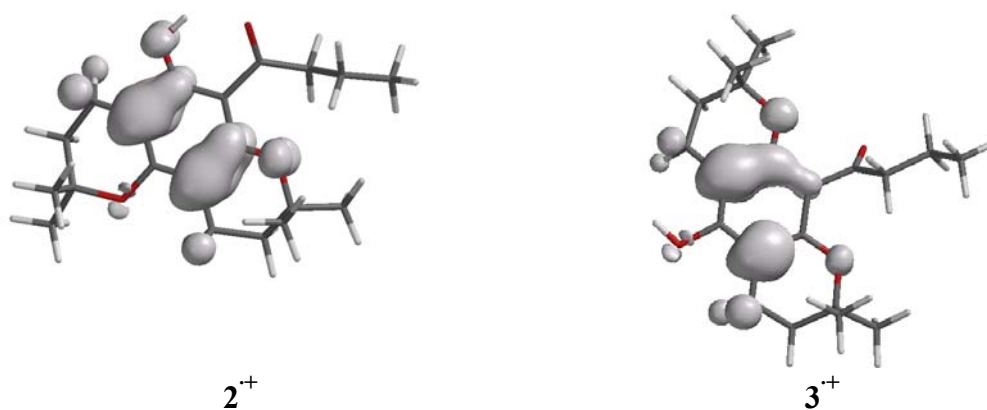


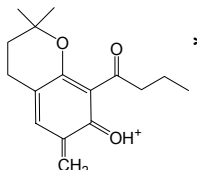
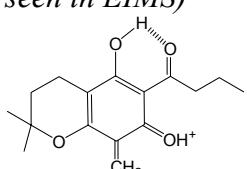
**Table 1.** EIMS fragments ( $m/z$ ) and their intensities (in %) for **2** and **3**.

$m/z$	<b>2</b>	<b>3</b>
332	70	18
289	53	100
277	100	5
261	40	4
233	9	70
230	49	-
221	52	10
203	17	3
177	39	31
109	18	12
81	13	6

These pronounced differences in the fragmentation of the two isomers prompted us to subject structures **2** and **3** to semi-empirical calculations (AM1), in an attempt to compare the predicted sites of ionization with their associated fragmentation patterns. In both molecules, however, the highest occupied molecular orbital (HOMO) energy that is represented by the reciprocal value of the ionization potential (Koopmans' theorem [15]) is located predominantly on the aromatic moiety (Figure 4). In addition, the spin density maps (Figure 5) for both radical cations **2**<sup>+</sup> and **3**<sup>+</sup>, which are generated from AM1 calculations by removing one electron from the corresponding parent molecules **2** and **3**, are located over the aromatic rings, in regions similar to those occupied by the HOMO energies of **2** and **3**. Thus, neither the HOMO nor the spin density maps provided a suitable explanation for the differences in the fragmentation patterns of **2** and **3**.

**Figure 4.** Orbital representation of the HOMO energies of **2** and **3**.

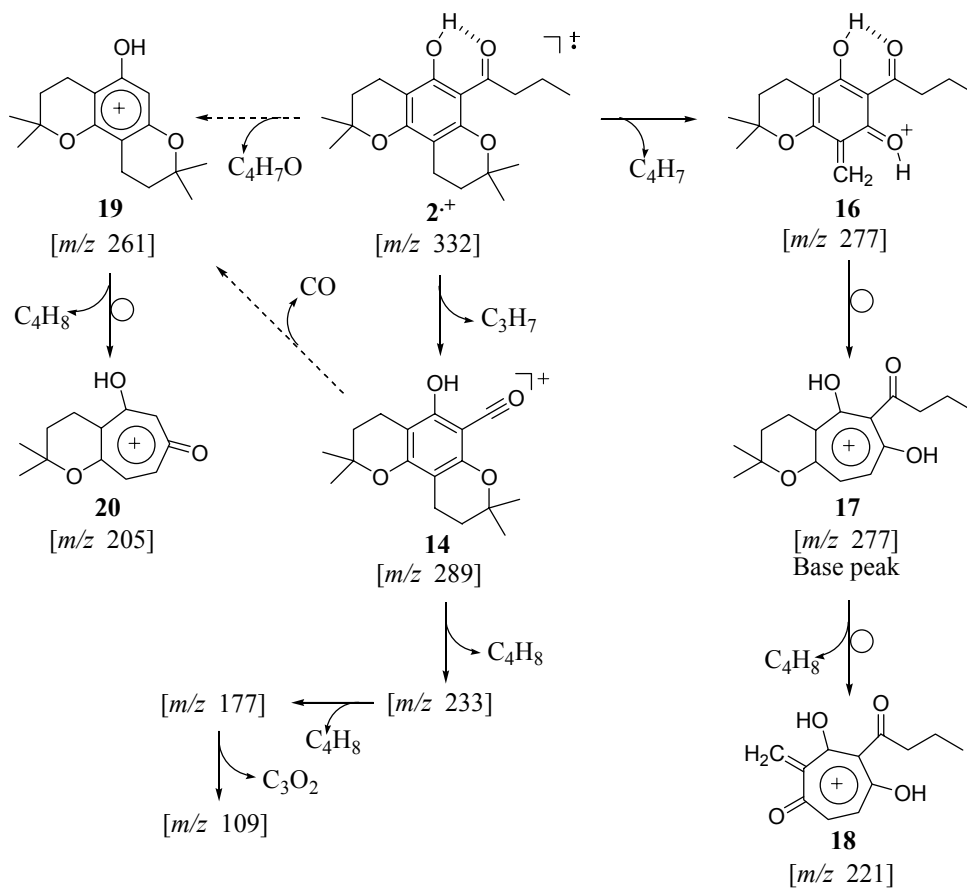
**Figure 5.** Spin density maps of the radical cations **2**<sup>•+</sup> and **3**<sup>•+</sup>.**Table 2.** AM1 relative energies (kcal.mol<sup>-1</sup>) calculated for **2** and **3** and select cationic species derived from these benzodipyrans. The relative energies for **16** and its analogous ion from the "linear" isomer (not seen in EIMS) are also shown for comparative purposes.

	<b>2</b>	<b>3</b>	$\Delta H_f^2 - \Delta H_f^3$
Parent compounds	-175.701	-170.990	-4.711
Radical cations	1.568	6.618	-5.050
Ar-C≡O: <sup>+</sup>	25.401	18.654	+6.747
		19.062	
<i>*derived from 3 (not seen in EIMS)</i>			
	12.856		-6.206

Since the semi-empirical calculations did not offer an explanation for the diverse fragmentation patterns of **2** and **3**, it was deemed appropriate to comparatively evaluate the relative energies (heat of formation  $\Delta H_f$ ) of the isomers **2** and **3**, their radical cations **2**<sup>•+</sup> and **3**<sup>•+</sup>, and the isomeric Ar-C≡O:<sup>+</sup> fragments **14** and **15** (see Schemes 3 and 4) that result from loss of the propyl group.

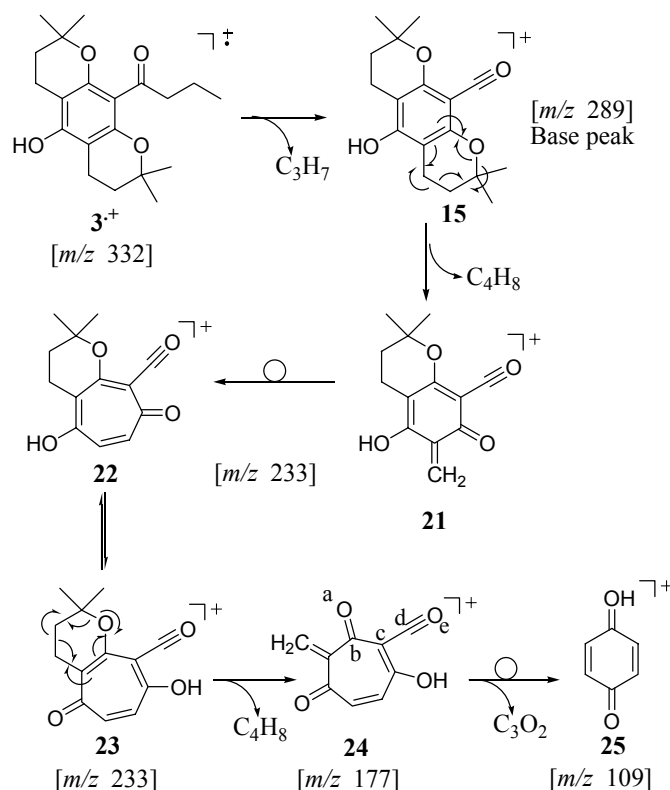
Because **2** and **3** are constitutional isomers their relative energies can be directly compared. The relative energies (Table 2) reveal that the "angular" benzodipyran **2** is more stable than its "linear" isomer **3** by ca. 5 kcal.mol<sup>-1</sup>. This energy advantage of **2** over **3** can easily be rationalized by the presence, in **2**, of hydrogen bonding between the C=O group and the adjacent OH (d = 1.997 Å between O and H), resulting in a reduction of the entropy and an increased stabilization of the molecule. This hydrogen bonding was also illustrated by <sup>1</sup>H NMR (Figure 1). An exchangeable phenolic proton signal was observed at 4.95 ppm (s, 1H) in the spectrum of **3**, but was absent in the spectrum of the "angular" isomer **2**. In **2**, this hydrogen bonding restricts the carbonyl group close to coplanarity ( $\theta = 27^\circ$ ) with the aromatic ring while in **3**, the carbonyl group opens to an angle of ca. 70° relative to the aromatic ring (see Figures 4 and 5). Thus, both the parent benzodipyran **2** and its radical cation **2**<sup>•+</sup> are more stable than **3** and its corresponding radical cation **3**<sup>•+</sup>. On the other hand, the Ar-C≡O:<sup>+</sup> fragment **14**, derived from **2**, is less stable than the Ar-C≡O:<sup>+</sup> fragment **15**, derived from **3**, by about 6.7 kcal.mol<sup>-1</sup>. This indicates that loss of the propyl group from radical cations **2**<sup>•+</sup> and **3**<sup>•+</sup> is disfavored by nearly 12 kcal.mol<sup>-1</sup> for isomer **2** relative to isomer **3**. Such an energy difference may account for partitioning to occur from radical cations **2**<sup>•+</sup> and **3**<sup>•+</sup> to yield fragments [Ar-C≡O:<sup>+</sup>] **14** and **15** at *m/z* 289 after loss of propyl or to the molecular ion at *m/z* 277 from loss of the [C<sub>4</sub>H<sub>7</sub>] fragment (55 amu) from the benzodipyran moiety (see Schemes 3 and 4).

**Scheme 3.** EI Induced fragmentation of the "angular" benzodipyran isomer **2**.



The fragmentation of **2** (Scheme 3) proceeds by partitioning of the radical cation  $2^+$  to lose propyl by  $\beta$  cleavage relative to the aromatic ring rendering cation **14** at  $m/z$  289 and by loss of a fragment (55 amu) resulting from the fragmentation of one of the chroman moieties and the transfer of a proton to the oxygen atom yielding molecular ion **16** at  $m/z$  277. Further fragmentation of **14** successively leads to fragment ions at  $m/z$  233,  $m/z$  177 and  $m/z$  109 (the same fragmentation pathway is observed with **15** as shown in Scheme 4 below). The fragment ion **16** most likely rearranges to the more stable hydroxytropylium ion **17** from which the second 2,2-dimethylpyran can fragment by loss of  $[\text{CH}_2=\text{C}(\text{CH}_3)_2]$  (56 amu) to yield the molecular ion **18** at  $m/z$  221. Fragment ion **19** at  $m/z$  261 most likely results from loss of the  $[\text{CO-propyl}]$  fragment (71 amu) directly from the parent ion  $2^+$  or sequentially from the fragment ion **14**. Fragmentation of the chroman moiety would account for the molecular ion cluster **20** at  $m/z$  203–205 in the EIMS of **2** (see Figure 3).

**Scheme 4.** EI Induced fragmentation of the "linear" benzodipyrans isomer **3**.



For the "linear" isomer **3**, the loss of the propyl to yield **15** is followed by successive loss of the two  $[\text{CH}_2=\text{C}(\text{CH}_3)_2]$  fragments (56 amu) from the two chroman moieties affording molecular ions **21** at  $m/z$  233 and **24** at  $m/z$  177, respectively (Scheme 4). In the fragmentation of **3**, however, the retro Diels-Alder rearrangements occur without proton transfer to the aromatic moiety. As previously discussed in the rearrangement of **1**, and reported for **4** [9], the quinone methide ion **21** presumably rearranges to a more stable tropylium ion **23**. A molecular ion at  $m/z$  109 (**25**, 12 % intensity) is likely to result from the loss of a  $[\text{C}_3\text{O}_2]$  fragment (68 amu). Although this  $\text{C}_3\text{O}_2$  fragment was not confirmed, the loss of atoms a–e from **24** may afford the stable protonated paraquinone molecular ion **25**.

## Conclusions

The striking differences in the fragmentation pathways of two isomeric phenolic tetramethyldichromans appear to be attributable to the presence or absence of hydrogen bonding in these molecules. Hydrogen bonding occurs between the aromatic hydroxyl group and the carbonyl moiety contained in an *ortho* phenone group present in the "angular" benzodipyran isomer **2**. The "linear" benzodipyran isomer **3** carries the aromatic hydroxyl group *para* to the phenone moiety, effectively precluding any intramolecular hydrogen bonding. The hydrogen bonding appears to assist electron-induced cleavage that occurs  $\beta$  to the aromatic ring both in the "angular" benzodipyran **2** and in 5,7-dihydroxy-2,2-dimethyl-8-butyryl chroman (**1**), a related monochroman that is also subject to hydrogen bond formation.

## Experimental

### General

Electron ionization mass spectrometry (EIMS) was performed on an AEI MS-12 computer coupled mass spectrometer at 70 eV. A scan range of 350–50 amu was used to acquire the MS data and 3 spectra were obtained for each compound. Nuclear magnetic resonance (NMR) spectra (see Figure 1) were recorded on a Bruker WP-80 spectrometer with tetramethylsilane (TMS) as the internal reference. Melting points (mp) were determined with a Reichert hot-stage apparatus and are uncorrected. Elemental analyses were performed on a Perkin-Elmer 240 analyzer. Preparative chromatography was carried out on a Waters/LC System 500 or on open columns packed with Silica Gel 60 (70-230 mesh; Merck & Co, Inc, Rahway, NJ). Calculations at the semiempirical level of theory were performed using the Austin Model-1 (AM1) [16] module contained in the SPARTAN '04 Windows software package (Wavefunction Inc, Irvine, CA). The restricted Hartree-Fock (RHF) approximation was used for closed-shell systems while unrestricted Hartree-Fock (UHF) was used for the calculation of radicals.

### Synthesis of 5,7-dihydroxy-2,2-dimethyl-8-butyryl chroman (**1**).

2-Butyryl-4-(3-methylbuten-2-yl)phloroglucinol (2 g) was prepared according to the literature [17,18] and suspended in benzene (25 mL). Trifluoroacetic acid (1.5 mL) was added and the mixture stirred for 6 hours at room temperature. The resulting solution was stripped to dryness under vacuum. The residue was chromatographed using 9:1 benzene/ethyl acetate, to yield chroman **1** in 70% yield as the compound (of two) with the longest column retention time (mp 102–104 °C; C, H analysis: calc for C<sub>15</sub>H<sub>20</sub>O<sub>4</sub>: 68.16, 7.63%; found: 67.97, 7.74%; M, 264, M<sup>+</sup>, 264; <sup>1</sup>H-NMR data as previously reported [2]. The isomeric 5,7-dihydroxy-2,2-dimethyl-8-butyryl chroman – the product with the shorter retention time – was not isolated due to very poor yield.

*Synthesis of the isomeric benzodipyran 2 and 3.*

A solution of 2-methyl-1,3-butadiene (6.1 g, 0.09 mol) in petroleum ether (bp 60–80 °C, 30 mL) was added to a solution of phlorobutyrophenone (prepared according to the Hoesch method [19], 11.8 g, 0.06 mol) in a mixture of ortho phosphoric acid (15 mL) and petroleum ether (bp 60–80 °C, 30 mL). The reaction mixture was stirred for 6 hours at 30–35 °C, then kept overnight at room temperature and finally diluted with diethyl ether (300 mL). The ether solution was washed with a saturated sodium carbonate solution (4 × 50 mL) then washed with water, dried over sodium sulfate and finally stripped to dryness under vacuum. The residue was chromatographed over silica gel (open column) eluting with 4:1 petroleum ether/ethyl acetate. The two benzodipyran **2** and **3** were isolated and further purified by recrystallization from benzene/petroleum ether: 6-butyryl-5-hydroxy-2,2,8,8-tetramethyl-3,4,9,10-tetrahydro-2H,8H-benzo[1,2-b:3,4-b<sup>1</sup>]dipyran (**2**) was the product with the highest R<sub>f</sub> value (~0.74) as assessed on TLC (silica gel; 4:1 petroleum ether/ethyl acetate) and was isolated in 30% yield (mp 79–81 °C; C, H analysis: calc for C<sub>20</sub>H<sub>28</sub>O<sub>4</sub>: 72.26, 8.49%; found: 72.23, 8.52%; M, 332, M<sup>+</sup>, 332) while 10-butyryl-5-hydroxy-2,2,8,8-tetramethyl-3,4,6,7-tetrahydro-2H,8H-benzo[1,2-b:5,4-b<sup>1</sup>]dipyran (**3**) was the product with the lowest R<sub>f</sub> value (~0.67) and was isolated in only 4% yield (mp 110–111 °C; C, H analysis: calc for C<sub>20</sub>H<sub>28</sub>O<sub>4</sub>: 72.26, 8.49%; found: 71.91, 8.63%; M, 332, M<sup>+</sup>, 332).

**References**

1. Bantick, J. R.; Cairns, H.; Chambers, A.; Hazard, R.; King, J.; Lee, T. B. Benzodipyran derivatives with antiallergic activity. *J. Med. Chem.* **1976**, *19*, 817-821.
2. Van der Schyf, C. J.; Dekker, T. G.; Fourie, T. G.; Snyckers, F. O. Synthesis and antimicrobial activity of a series of caespitin derivatives. *Antimicrob. Agents Chemother.* **1986**, *30*, 375-381.
3. Benbrook, D. M.; Madler, M. M.; Spruce, L. W.; Birckbichler, P. J.; Nelson, E. C.; Subramanian, S.; Weerasekare, G. M.; Gale, J. B.; Patterson, M. K.; Wang, B. H.; Wang, W.; Lu, S. N.; Rowland, T. C.; DiSivestro, P.; Lindamood, C.; Hill, D. L.; Berlin, K. D. Biologically active heteroarotinoids exhibiting anticancer activity and decreased toxicity. *J. Med. Chem.* **1997**, *40*, 3567-3583.
4. Ueno T, Takahashi H, Oda M, Mizunuma M, Yokoyama A, Goto Y, Mizushima Y, Sakaguchi K, Hayashi H. Inhibition of human telomerase by rubromycins: implication of spiroketal system of the compounds as an active moiety. *Biochemistry* **2000**, *39*, 5995-6002.
5. Hirota, M.; Miyazaki, S.; Minakuchi, T.; Takagi, T.; Shibata, H. Myrsinoic acids B, C and F, anti-inflammatory compounds from *Myrsine seguinii*. *Biosci. Biotechnol. Biochem.* **2002**, *66*, 655-659.
6. Rovnyak, G. C.; Ahmed, S. Z.; Ding, C. Z.; Dzwonczyk, S.; Ferrara, F. N.; Humphreys, W. G.; Grover, G. J.; Santafianos, D.; Atwal, K. S.; Baird, A. J.; McLaughlin, L. G.; Normandin, D. E.; Sleph, P. G.; Traeger, S. C. Cardioselective antiischemic ATP-sensitive potassium channel (KATP) openers. 5. Identification of 4-(N-aryl)-substituted benzopyran derivatives with high selectivity. *J. Med. Chem.* **1997**, *40*, 24-34.

7. Cho, H.; Katoh, S.; Sayama, S.; Murakami, K.; Nakanishi, H.; Kajimoto, Y.; Ueno, H.; Kawasaki, H.; Aisaka, K.; Uchida, I. Synthesis and selective coronary vasodilatory activity of 3,4-dihydro-2,2-bis(methoxymethyl)-2H-1-benzopyran-3-ol derivatives: novel potassium channel openers. *J. Med. Chem.* **1996**, *39*, 3797-3805.
8. Comoy, C.; Marot, C.; Podona, T.; Baudin, M. L.; MorinAllory, L.; Guillaumet, G.; Pfeiffer, B.; Caignard, D. H.; Renard, P.; Rettori, M. C.; Adam, G.; GuardiolaLemaitre, B. 3-amino-3,4-dihydro-2H-1-benzopyran derivatives as 5-HT<sub>1A</sub> receptor ligands and potential anxiolytic agents. 2. Synthesis and quantitative structure-activity relationship studies of spiro[pyrrolidine- and piperidine-2,3'(2'H)-benzopyrans] *J. Med. Chem.* **1996**, *39*, 4285-4298.
9. Willhalm, B.; Thomas, A. F.; Gautschi, F. Mass spectra and organic analysis – III. Mass spectra of aromatic ethers in which the oxygen forms part of a ring. *Tetrahedron* **1964**, *20*, 1185-1209.
10. Trudell, J. R.; Sample Woodgate, S. D.; Djerassi, C. Mass spectrometry in structural and stereochemical problems – CLXXXVII. A study of skeletal rearrangements in chromans by combined <sup>13</sup>C and deuterium labeling. *Org. Mass Spectrom.* **1970**, *3*, 753-776.
11. Hiessbock, R.; Wolf, C.; Richter, E.; Hitzler, M.; Chiba, P.; Kratzel, M.; Ecker, G. Synthesis and in vitro multidrug resistance modulating activity of a series of dihydrobenzopyrans and tetrahydroquinolines. *J. Med. Chem.* **1999**, *42*, 1921-1926.
12. Dalluge, J. J.; Nelson, B. C. Determination of tea catechins. *J. Chromatogr. A.* **2000**, *881*, 411-424.
13. Setchell, K. D.; Zimmer-Nechemias, L.; Cai, J.; Heubi, J. E. Isoflavone content of infant formulas and the metabolic fate of these phytoestrogens in early life. *Am. J. Clin. Nutr.* **1998**, *68*, 1453S-1461S.
14. Setchell, K. D.; Brown, N. M.; Lydeking-Olsen, E. The clinical importance of the metabolite equol - a clue to the effectiveness of soy and its isoflavones. *J. Nutr.* **2002**, *132*, 3577-3584.
15. Koopmans, T. Ordering of wave functions and eigenenergies to the individual electrons of an atom. *Physica* **1934**, *1*, 104-113.
16. M. J. S. Dewar; E. G. Zoebisch; E. F. Healy; J. J. P. Stewart Austin Model 1, newly parametrized MNDO version. *J. Am. Chem. Soc.* **1985**, *107*, 3902-3909.
17. Dekker, T. G.; Fourie, T. G.; Naudé, M. U.; Snyckers, F. O.; Van der Schyf, C. J. A convenient preparation of alkenylated acylphloroglucinols. *S. Afr. J. Chem.* **1984**, *37*, 74-75.
18. Dekker, T. G.; Fourie, T. G.; Snyckers, F. O.; Van der Schyf, C. J. <sup>13</sup>C NMR spectra of 3-substituted phlorophenone compounds. *Org. Magn. Reson.* **1984**, *22*, 607-608.
19. Hoesch, K. Synthesis of acylphenols from phenols or phenolic ethers. (Ger.). *Chem. Ber.* **1915**, *48*, 1122-1133.

*Sample availability:* Contact the corresponding author.